On Achievable Rates in Massive MIMO-based Hexagonal Cellular System with Pilot Contamination

Zaka ul Mulk and Syed Ali Hassan
School of Electrical Engineering & Computer Science (SEECS)
National University of Sciences & Technology (NUST), Islamabad, Pakistan 44000
Email: {12mseezmulk, ali.hassan}@seecs.edu.pk

***Abstract*—In this paper, a pilot reuse scheme is considered for the uplink of a massive multiple input multiple output (MIMO) system and a lower bound on the throughput of the system is derived, which is applicable for any number of antennas. A hexagonal geometry of the system is considered where each cell contains uniformly distributed users and a conventional frequency reuse pattern. The derived lower bound is shown to be limited by three types of interferences: inter-cell interference, intra-cell interference and pilot contamination. A set of conditions including the number of users, antennas, pilot reuse factor and coherence period is analyzed for which the lower bound of throughput is achieved. The results indicate that the reuse factor plays a critical role in the least achievable throughput. A minimum reuse factor is quantified for a given user density and coherence period.**

***Index Terms*—Multiuser MIMO, pilot contamination, pilot reuse factor, channel estimation.**

I. Introduction

In wireless cellular systems, multiple antennas are used at the base station (BS), which provide high throughput as well as improved quality of service to its users. Considering a multiple cell geometry, where each cell is equipped with tens of antenna making a massive MIMO system, it is obvious that the knowledge of channel state information (CSI) at the base station plays an important role to achieve high system performance. The most efficient way of obtaining CSI is through reciprocity that uses uplink training of pilots [1],[2]. The major constraint while considering a multiple cell scenario is the allocation of pilot signals to the users. This affects the system performance in a great way as the CSI is further dependent upon the pilot allocation scheme. The frequent mobility of users shortens the channel coherence period and as a result the length of pilot sequence gets limited. Therefore, considering the scarcity of bandwidth it is not feasible to allocate distinct orthogonal pilot signals to users in each cell. The major issue of reusing non-orthogonal pilot signals in different cells is commonly known as pilot contamination that limits the achievable throughput [3]. It is caused when the CSI at BS is corrupted because of pilot signals from neighboring cells using the same frequency.

Marzetta [4] has shown in his work that as the number of antennas increases to infinity, the throughput eventually saturates. Gopalakrishnan et al. [5] and Ngo et al. [6] derived the asymptotic throughput bound, which shows that the throughput is limited by pilot contamination. Different techniques have been studied in order to reduce the effect of pilot contamination. Tadilo et al. [7] proposed a novel pilot optimization and channel estimation algorithm to reduce the weighted sum mean square error (WSMSE). Papadopoulos et al. [8] and Huh et al. [9] improved the throughput with the help of cooperative communication in which they divided the mobile terminals in different groups. Appaiah et al. [10] used asynchronous transmission of pilots to reduce the correlation error for channel estimation and Jose et al. [3] worked on regularized zero force precoding. Yang et al. [11] derived the throughput for a line geometry of cells where users are co-located in each cell.

In this paper, a regular hexagonal geometry with random deployment of users is considered in order to study the impact of pilot contamination for a more general scenario. Specifically, we study a conventional frequency reuse hex geometry and derive the throughput of the network when multiple users are reusing the same pilots leading to pilot contamination problem. We restrict ourselves to only first tier of co-channel interferers. Finally, with the help of numerical simulations, relations among cell throughput, numbers of antennas, number of users per cell, pilot reuse factor and coherence period have been studied. It is shown that the reuse pattern has strong impact on the system achievable throughput.

The rest of the paper is organized as follows. In Section II, the system model is discussed. In Section III, lower bound for achievable cell throughput is derived and different interference terms are analyzed. In Section IV, the numerical results for average cell throughput and other parameters are discussed. Finally, we draw conclusions in Section V.

II. System Model

Consider a tier-1 hexagonal geometry of a cellular system, where each cell has a radius R. By tier-1 we refer to the area of interfering cells that causes co-channel interference (CCI) and is considered the main source of pilot contamination. The reuse factor of the hexagonal geometry is given by Q, where $Q = \{1, 3, 4, 7, ...\}$. For instance, in Fig. 1, six interfering cells for the center cell constitute tier-1 geometry with Q=1.

978-1-4799-8088-8/15/$31.00 ©2015 IEEE

Each cell contains an M-antenna base station (BS) that serves K randomly deployed single antenna mobiles. Let $d_{i,j,k}$ be the distance between user k of cell j and the BS antennas of cell i, then the path loss factor is given by

$$\varphi_{i,j,k} = \frac{1}{d_{i,j,k}^{\alpha}} \tag{1}$$

where α is the path loss exponent. Although the distance to all BS antennas potentially remains the same for one user, however, we will use this notation for consistency with fading gains.

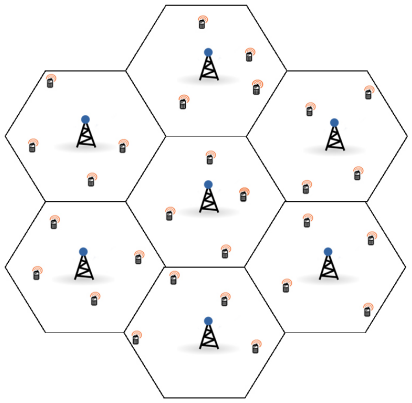

Fig. 1: Random deployment of users in a hexagonal geometry with Q = 1

A Rayleigh block fading channel is assumed where all the channel coefficients remain constant for a block of T symbols; T being the channel coherence period. Considering the geometry, the channel matrix between the antenna i and mobiles in cell j is $\mathbf{C}_{i,j} \in \mathcal{C}^{M\times K}$ where all the entries of $\mathbf{C}_{i,j}$ are independent and identically distributed (i.i.d.) complex Gaussian with zero mean and unit variance.

III. Multi-cell Uplink Communication

All the mobiles in this uplink scenario communicate with their respective base station in two stages: uplink training with pilot reuse and actual transmission of the data.

A. Uplink Training with Pilot Reuse

In each cell, orthogonal pilots are assigned to the users, which are reused by other cells by the factor Q. Assume a pre-designed pilot sequence matrix

$$\mathbf{\Psi} = [\Psi_0, \cdots, \Psi_{Q-1}] \qquad \in \mathbb{C}^{QK\times QK} \tag{2}$$

where $\mathbf{\Psi}$ is divided among all cells. Assume that Ψ_0 is assigned to the Cell 0 which is considered to be the serving cell (center cell from Fig. 1) and the pilot sequence is further reused by Cell lQ where $1 \leq |l| \leq \lfloor \frac{L}{Q} \rfloor$ where L is the total number of cells in geometry. The pilot $\Psi_{q,k}$ is assigned to a single user k of a cell in order to remove intra-cell interference with the help of orthogonality of pilot signals.

We only analyze Cell 0 here for brevity. In a single time-frequency block, all the mobiles send their pilot signals to the base station. The signals received at base station 0 are

$$\mathbf{P}_0 = \sqrt{\phi_\tau QK} \sum_{j=0}^{L-1} \mathbf{C}_{0,j}\ \Psi^*_{(j)} + \mathbf{W}_0, \qquad \in \mathbb{C}^{M\times K} \tag{3}$$

where $\mathbf{C}_{0,j} = [\varphi_{0,j,1}\mathbf{c}_{0,j,1}, \cdots, \varphi_{0,j,K}\mathbf{c}_{0,j,K}]$ is the channel matrix between the mobiles of cell j and base station 0, $\mathbf{c}_{0,j,k}$ is the channel vector between base station 0 and cell $j's$ k-th mobile user and $(j) = (j \mod Q)$. The variable $\mathbf{W}_0$ is i.i.d. $\mathcal{CN}(0,1)$ and ϕ_τ is the average transmission power per mobile. The factor $\sqrt{QK}$ guarantees that average power is ϕ_τ.

The received signal $\mathbf{P}_0$ is projected onto $\Psi_{0,k}$ in order to estimate $\mathbf{c}_{0,0,k}$ at the base station 0. After normalization, the resulting signals are

$$\overline{\mathbf{p}}_{0,k} = \mathbf{c}_{0,0,k} + \sum_{l\neq 0} \sqrt{\frac{\varphi_{0,lQ,k}}{\varphi_{0,0,k}}}\mathbf{c}_{0,lQ,k} + \frac{\mathbf{w}_{0,k}}{\sqrt{\varphi_{0,0,k}\phi_\tau KQ}} \ \in \mathbb{C}^{M\times 1}. \tag{4}$$

A minimum mean squared error (MMSE) estimator [12] is applied to the received vector of pilots to get

$$\hat{\mathbf{c}}_{0,0,k} = \mathbf{Y}_{cp}\mathbf{Y}_{pp}^{-1}\overline{\mathbf{P}}_{0,k}; \tag{5}$$

where $\mathbf{Y}_{pp}$ and $\mathbf{Y}_{cp}$ are the correlation and cross-correlation matrices, respectively. As all the channel vectors are independent therefore, the cross-correlation matrix becomes $\mathbf{Y}_{cp} = \mathbf{I}_M$. The correlation matrix $\mathbf{Y}_{pp}$ is given as

$$\mathbf{Y}_{pp} = \mathbf{I}_M + \underbrace{\sum_{l\neq 0} \frac{\varphi_{0,lQ,k}}{\varphi_{0,0,k}}}_{a_1}\mathbf{I}_M + \underbrace{\frac{1}{\varphi_{0,0,k}\ \phi_\tau KQ}}_{a_2}\mathbf{I}_M. \tag{6}$$

From the above equation, we can define $\sigma_\tau^2 = (1+a_1+a_2)^{-1}$ and now applying the MMSE decomposition

$$\mathbf{c}_{0,0,k} = \hat{\mathbf{c}}_{0,0,k} + \tilde{\mathbf{c}}_{0,0,k}, \tag{7}$$

where $\tilde{\mathbf{c}}_{0,0,k}$ is the independent uncorrelated estimation error. Both the entries are i.i.d. where $\hat{\mathbf{c}}_{0,0,k}$ is $\mathcal{CN}(0,\sigma_\tau^2)$ and $\tilde{\mathbf{c}}_{0,0,k}$ is $\mathcal{CN}(0,1-\sigma_\tau^2)$.

B. Actual Transmission of Data

In the next $T - KQ$ slots, all the mobiles transmit their data. This takes place in all cells after the uplink training of pilots. The received signal at base station 0 is

$$\mathbf{r_0} = \sum_{j,k} \sqrt{\phi\varphi_{\mathbf{0},j,k}}\ \mathbf{c_0}_{,j,k}\ r_{j,k} + \mathbf{n_0}, \tag{8}$$

where ϕ is the average power consumed by a mobile to transmit the data $r_{j,k}$ by a user k in cell j and $\mathbf{n}_o$ is the noise, which is $\mathcal{CN}(0,1)$. At base station 0, maximum ratio combining (MRC) is applied to receive the k-th mobile's signal. The unit norm vector is denoted as

$$\mathbf{u}_k = \frac{\hat{\mathbf{c}}_{0,0,k}}{\|\hat{\mathbf{c}}_{0,0,k}\|} \qquad \in \mathbb{C}^{M\times 1}. \tag{9}$$

After applying maximum ratio combining and normalization, we get

$$\mathbf{u}_k^*\bar{\mathbf{r}}_0 = \mathbf{u}_k^*\hat{\mathbf{c}}_{0,0,k}\ r_{0,k} + \sqrt{\frac{1}{\phi_\tau \varphi_{0,0,k}}}w_k \tag{10}$$

$$+ \mathbf{u}_k^*\tilde{\mathbf{c}}_{0,0,k}\ r_{0,k} + \mathbf{u}_k^*\sum_{i\neq k}\sqrt{\frac{\varphi_{0,0,i}}{\varphi_{0,0,k}}}\mathbf{c}_{0,0,i}r_{0,i} \tag{10a}$$

$$+ \mathbf{u}_k^*\sum_{j\neq 0}\sum_{i=1}^{K}\sqrt{\frac{\varphi_{0,j,i}}{\varphi_{0,0,k}}}\mathbf{c}_{0,j,i}r_{j,i}. \tag{10b}$$

In (10), the two terms are desired signal and the noise respectively. In (10a) the terms refer to intra-cell interference and in (10b) the term denotes inter-cell interference.

C. Achievable Cell Throughput

The average throughput of cell 0 using the above mentioned scheme is achieved by the following derivation. Tier-1 base stations of hexagonal geometry with M-antenna are deployed. Each base station serves K randomly located single antenna mobiles of its own cell with path loss factor $\varphi_{0,0,k}$. The inter cell interference in equation (10b) can be re-written as

$$\mathbf{u}_k^*\sum_{j\neq 0}\sum_{i=1}^{K}\sqrt{\frac{\varphi_{0,j,i}}{\varphi_{0,0,k}}}\mathbf{c}_{0,j,i}r_{j,i} - \mathbf{u}_k^*\sum_{l\neq 0}\sqrt{\frac{\varphi_{0,lQ,k}}{\varphi_{0,0,k}}}\mathbf{c}_{0,lQ,k}r_{lQ,k} \tag{11}$$

$$+\mathbf{u}_k^*\sum_{l\neq 0}\sqrt{\frac{\varphi_{0,lQ,k}}{\varphi_{0,0,k}}}\mathbf{c}_{0,lQ,k}r_{lQ,k}, \tag{11a}$$

where (11a) represents the pilot contamination. For a single user k, we can calculate the throughput as

$$\mathcal{R} \geq \log\left(1 + \frac{|\mathbf{u}_k^*\hat{\mathbf{c}}_{0,0,k}|^2}{\frac{1}{\phi\varphi_{0,0,k}} + I_1 + I_2 + I_3}\right), \tag{12}$$

where I_1, I_2, I_3 are intra-cell, inter-cell and interference due to pilot contamination, respectively and given as

$$I_1 = |\mathbf{u}_k^*\tilde{\mathbf{c}}_{0,0,k}|^2 + \sum_{i\neq k}\left|\mathbf{u}_k^*\sqrt{\frac{\varphi_{0,0,i}}{\varphi_{0,0,k}}}\mathbf{c}_{0,0,i}\right|^2, \tag{13}$$

$$I_2 = \sum_{j\neq 0}\sum_{i=1}^{K}\frac{\varphi_{0,j,i}}{\varphi_{0,0,k}}|\mathbf{u}_k^*\mathbf{c}_{0,j,i}|^2 - \sum_{l\neq 0}\frac{\varphi_{0,lQ,k}}{\varphi_{0,0,k}}|\mathbf{u}_k^*\mathbf{c}_{0,lQ,k}|^2, \tag{14}$$

$$I_3 = \sum_{l\neq 0}\frac{\varphi_{0,lQ,k}}{\varphi_{0,0,k}}|\mathbf{u}_k^*\mathbf{c}_{0,lQ,k}|^2. \tag{15}$$

Both the terms I_1 and I_2 are independent of $|\mathbf{u}_k^*\hat{\mathbf{c}}_{0,0,k}|^2$, whereas I_3 is dependent upon $\mathbf{c}_{0,0,k}$ which also shows dependence upon $|\mathbf{u}_k^*\hat{\mathbf{c}}_{0,0,k}|^2$. In order to analyze I_3, MMSE decomposition is applied on $\mathbf{c}_{0,lQ,k}$. Hence we can write $\hat{\mathbf{c}}_{0,lQ,k}$ as $\hat{\mathbf{c}}_{0,0,k}$ because the MMSE decomposition for both the terms is proportional. Thus,

$$\mathbf{c}_{0,lQ,k} = \sqrt{\frac{\varphi_{0,lQ,k}}{\varphi_{0,0,k}}}\hat{\mathbf{c}}_{0,0,k} + \tilde{\mathbf{c}}_{0,lQ,k}, \tag{16}$$

where $\tilde{\mathbf{c}}_{0,lQ,k}$ is i.i.d. $\mathcal{CN}(0, 1 - \frac{\varphi_{0,lQ,k}}{\varphi_{0,0,k}}\sigma_\tau^2)$ and denotes the estimation error and is not dependent upon $\hat{\mathbf{c}}_{0,lQ,k}$. Re-write I_3 as

$$I_3 = \sum_{l\neq 0}\frac{\varphi_{0,lQ,k}^2}{\varphi_{0,0,k}^2}|\mathbf{u}_k^*\hat{\mathbf{c}}_{0,0,k}|^2 + \sum_{l\neq 0}\frac{\varphi_{0,lQ,k}}{\varphi_{0,0,k}}|\mathbf{u}_k^*\tilde{\mathbf{c}}_{0,lQ,k}|^2$$
$$+ \sum_{l\neq 0}\left((\frac{\varphi_{0,lQ,k}}{\varphi_{0,0,k}})^{\frac{3}{2}}(\mathbf{u}_k^*\hat{\mathbf{c}}_{0,0,k}\tilde{\mathbf{c}^*}_{0,lQ,k}\mathbf{u}_k + \mathbf{u}_k^*\tilde{\mathbf{c}}_{0,lQ,k}\hat{\mathbf{c}^*}_{0,0,k}\mathbf{u}_k)\right), \tag{17}$$

and denote the rate conditioned on $\hat{\mathbf{c}}_{0,0,k}^*$ by $\bar{\mathcal{R}}$. To achieve the lower bound of $\bar{\mathcal{R}}$, convexity of $\log(1+\frac{1}{x})$ is used, therefore,

$$\bar{\mathcal{R}} \geq \log\left(1 + \frac{|\mathbf{u}_k^*\hat{\mathbf{c}}_{0,0,k}|^2}{\frac{1}{\phi\varphi_{0,0,k}} + \mathbb{E}[I_1] + \mathbb{E}[I_2] + \mathbb{E}[I_3]}\right) \tag{18}$$

where $\mathbb{E}[I_1], \mathbb{E}[I_2]$ and $\mathbb{E}[I_3]$ are given as

$$\mathbb{E}[I_1] = (1-\sigma_\tau^2) + \sum_{i\neq k}\frac{\varphi_{0,0,i}}{\varphi_{0,0,k}} \tag{19}$$

$$\mathbb{E}[I_2] = \sum_{j\neq 0}\sum_{i=1}^{K}\frac{\varphi_{0,j,i}}{\varphi_{0,0,k}} - \sum_{l\neq 0}\frac{\varphi_{0,lQ,k}}{\varphi_{0,0,k}} \tag{20}$$

$$\mathbb{E}[I_3] = \sum_{l\neq 0}\frac{\varphi_{0,lQ,k}^2}{\varphi_{0,0,k}^2}|\mathbf{u}_k^*\hat{\mathbf{c}}_{0,0,k}|^2 + \sum_{l\neq 0}\frac{\varphi_{0,lQ,k}}{\varphi_{0,0,k}}(1 - \frac{\varphi_{0,lQ,k}}{\varphi_{0,0,k}}\sigma_\tau^2). \tag{21}$$

The last two terms in (17) have zero mean hence neglected in (21). Note that

$$|\mathbf{u}_k^*\hat{\mathbf{c}}_{0,0,k}|^2 = \sum_{q=1}^{M}\hat{c}_{k,q}^2, \tag{22}$$

where the term $\hat{c}_{k,q}$ is i.i.d. $\mathcal{CN}(0,\sigma_\tau^2)$. Hence, $|\mathbf{u}_k^*\hat{\mathbf{c}}_{0,0,k}|^2$ has Gamma distribution with parameters (M,σ_τ^2). The right hand side of (18) is written as

$$\log\left(1 + \frac{\Gamma_k}{\frac{1}{\phi\varphi_{0,0,k}} + \Omega_1 + \Omega_2 + \sum_{l\neq 0}\frac{\varphi_{0,lQ,k}^2}{\varphi_{0,0,k}^2}\Gamma_k}\right), \tag{23}$$

where $\Gamma_k = |\mathbf{u}_k^*\hat{\mathbf{c}}_{0,0,k}|^2$, Ω_1 is the intra-cell interference and Ω_2 is the inter-cell interference given as

$$\Omega_1 = (1-\sigma_\tau^2) + \sum_{i\neq k}\frac{\varphi_{0,0,i}}{\varphi_{0,0,k}}, \tag{24}$$

$$\Omega_2 = \sum_{j\neq 0}\sum_{i=1}^{K}\frac{\varphi_{0,j,i}}{\varphi_{0,0,k}} - \sum_{l\neq 0}\frac{\varphi_{0,lQ,k}^2}{\varphi_{0,0,k}^2}\sigma_\tau^2. \tag{25}$$

The inverse Gamma distribution $(1/\Gamma_k)$ has a mean value of $1/(M-1)\sigma_\tau^2$. Therefore,

$$\mathcal{R}_k \geq \log\left(1+\frac{1}{(\frac{1}{\phi\varphi_{0,0,k}}+\Omega_1+\Omega_2)/\Gamma_k+\sum_{l\neq 0}\frac{\varphi^2_{0,lQ,k}}{\varphi^2_{0,0,k}}}\right) \tag{26}$$

$$\geq \log\left(1+\frac{1}{(\frac{1}{\phi\varphi_{0,0,k}}+\Omega_1+\Omega_2)/\mathbb{E}\left[\frac{1}{\Gamma_k}\right]+\sum_{l\neq 0}\frac{\varphi^2_{0,lQ,k}}{\varphi^2_{0,0,k}}}\right) \tag{27}$$

$$\geq \log\left(1+\frac{(M-1)\sigma_\tau^2}{(\frac{1}{\phi\varphi_{0,0,k}}+\Omega_1+\Omega_2+\Omega_3}\right) \tag{28}$$

where $\Omega_3 = (M-1)\sum_{l\neq 0}\frac{\varphi^2_{0,lQ,k}}{\varphi^2_{0,0,k}}\sigma_\tau^2$ is the pilot contamination.

The average achievable throughput for cell 0 is given by

$$\mathcal{R} \geq K(1-\frac{QK}{T})\log\left(1+\frac{(M-1)\sigma_\tau^2}{\frac{1}{\phi\varphi_{0,0,k}}+\Omega_1+\Omega_2+\Omega_3}\right), \tag{29}$$

where ϕ is the average data power, T is the channel coherence period and σ_τ^2 is the normalized estimation power

$$\sigma_\tau^2 = \left(1+\sum_{l\neq 0}\frac{\varphi_{0,lQ,k}}{\varphi_{0,0,k}}+\frac{1}{\sqrt{\phi_\tau KQ}}\right)^{-1}. \tag{30}$$

In (29) the constants Ω_1, Ω_2 and Ω_3 are defined as

$$\begin{aligned}\Omega_1 &= (1-\sigma_\tau^2)+\sum_{i\neq k}\frac{\varphi_{0,0,i}}{\varphi_{0,0,k}},\\ \Omega_2 &= \sum_{j\neq 0}\sum_{i=1}^{K}\frac{\varphi_{0,j,i}}{\varphi_{0,0,k}}-\sum_{l\neq 0}\frac{\varphi^2_{0,lQ,k}}{\varphi^2_{0,0,k}}\sigma_\tau^2,\\ \Omega_3 &= (M-1)\sigma_\tau^2\sum_{l\neq 0}\frac{\varphi^2_{0,lQ,k}}{\varphi^2_{0,0,k}}.\end{aligned} \tag{31}$$

IV. Numerical Results

In this section, we evaluate the effect of different interferences, pilot reuse factor and network topology on the average cell throughput. Different simulations have been carried out to study the parameters upon which maximum throughput is achieved. For all simulations, we assume coherence period T = 100ms, radius R = 1.4km, path loss exponent α = 3.8 and ϕ_τ = ϕ = 100mW, unless noted otherwise. All the mobiles operate at 3GHz frequency and 10MHz bandwidth. In order to get ergodic cell throughput, $Monte\text{-}Carlo$ method is applied with 1e6 simulations for a single user having random location in every trial.

Fig. 2 shows the average throughput of the system versus the number of users. We can observe the dependence of throughput on the reuse factor and the number of users per cell. Average throughput of a cell increases when the number of users increases. Similarly $\mathcal{R}$ increases as the reuse factor goes from 1 to 7 because the pilot contamination decreases when the interfering mobiles get far away from the serving cell 0's base station. On the contrary, inter-cell and intra-cell interference have no effect with the change in Q but both interferences tend to increase with increasing K. The gain overcomes the loss due to both interferences hence the final net result is the increase in average throughput of a cell.

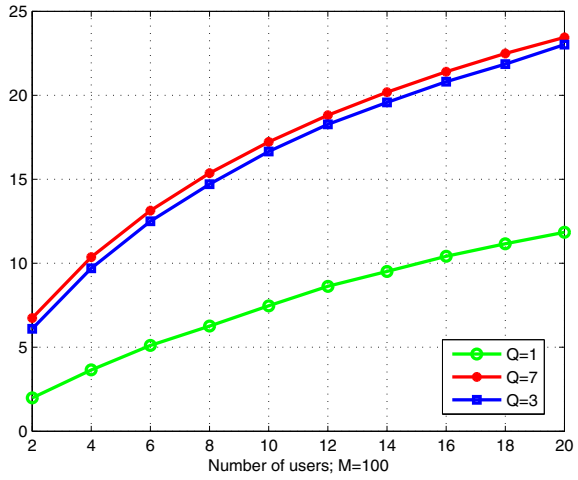

Fig. 2: Average throughput with different number of users and reuse factor

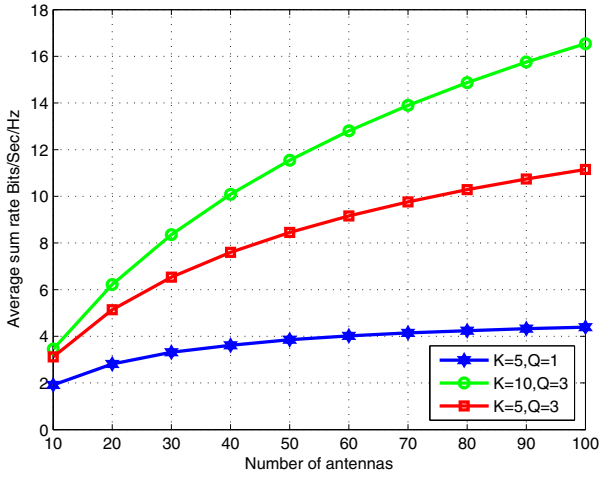

Fig. 3: Average throughput with different number of antennas

Fig. 3 depicts the relation between number of antennas and the average throughput for different reuse factor. The average sum-rate increases as the number of antennas increase. The saturation in throughput is not obvious for 100 antennas for reuse factor 3 as the interference power caused by pilot contamination using Q=3 is very small, whereas, the throughput saturates for higher number of antennas at reuse factor 1. Hence we can say that pilot contamination almost vanishes

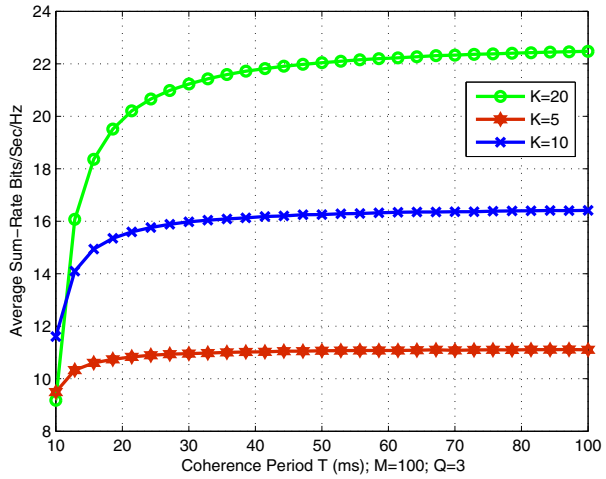

Fig. 4: Average throughput with coherence period and different number of users

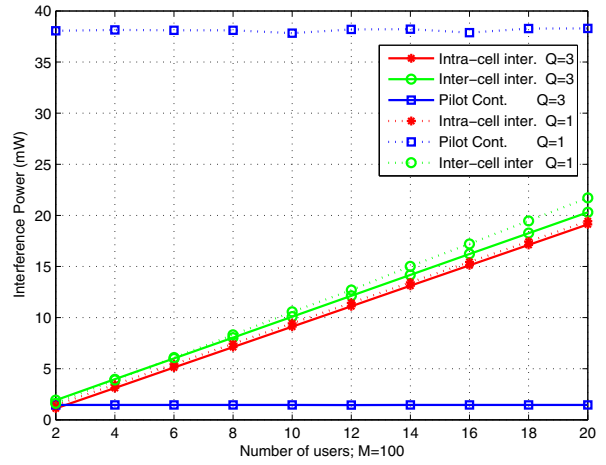

Fig. 5: Interference types with reuse factor and different number of users

for higher reuse factors.

Fig. 4 shows the relation between coherence period T and the average throughput with different number of mobiles K. When we consider only 5 users in a cell, the throughput doesn't change much with the increase in T but when K goes to 20, the throughput starts increasing gradually as T increases. It can be seen that for lower T, K=20 has the least performance. This is because, it is very difficult to generate orthogonal pilots for more users in lesser coherence period and hence the pilot contamination dominates the system. When T increases beyond a specific value, K=20 outperforms the rest of two cases.

Fig. 5 shows the dependence of different interference components upon the reuse factor and the number of users. As the number of users increases the inter-cell and intra-cell interference increase, whereas, the pilot contamination stays constant because for tier-1, the number of interferers causing pilot contamination will always be six for any reuse factor. On the average, the inter-cell and intra-cell interferences have the same impact on the throughput because the location of user is random; for distances closer to the base station, the intra-cell interference dominates and for distances far away, the inter-cell interference dominates. Hence, on the average, both contribute the same to the cell throughput.

V. Conclusion

In this paper, we evaluated the lower bound for non-asymptotic throughput of an uplink massive MIMO system with hexagonal geometry and random deployment of users. It was observed that the effect of pilot contamination diminishes when we have reuse factor greater than 1. Moreover, relationship between the number of users in a cell, number of base station antennas, duration of coherence period and average cell throughput has been studied through simulations. Through these studies, we can calculate the lower bound of average throughput for a cell that can be achieved for the different values of parameters like K,T,Q and M. We quantified the cell throughput for various reuse factors and showed that by moving to higher reuse factors, pilot contamination is reduced, however, there is very little or no effect on the inter-cell and intra-cell interference. We considered only MRC receivers, however in future we intend to also look into the MMSE receivers.

References

[1] T. L. Marzetta and B. M. Hochwald, "Fast transfer of channel state information in wireless systems," *IEEE Trans. Signal Process.,* vol.54, pp. 1268-1278, 2006.

[2] L. Lu, G. Y. Li, A. L. Swindlehurst, A. Ashikhmin, and R. Zhang, "An overview of massive MIMO: Benets and challenges," *IEEE J. Sel Topics Signal Process.,* April 2014.

[3] J. Jose, A. Ashikhmin, T. L. Marzetta and S. Vishwanath. "Pilot contamination problem in multi-cell TDD systems," *IEEE International Symposium on Information Theory,* pp 2184-2188, July, 2009.

[4] T. L. Marzetta "Noncooperative cellular wireless with unlimited number of base station antenna," *IEEE Trans. Wireless Commun.*, vol. 9, no. 11, pp. 3590-3600, Nov. 2010.

[5] B. Gopalkrishnan and N. Jindal, "An analysis of pilot contamination on Multi-user MIMO cellular systems with many antennas," *IEEE SPAWC*, pp. 381-385, June 2011.

[6] H. Q. Ngo, T.L.Marzetta and E.G.Larsson "Analysis of pilot contamination effect in very large multicell multiuser MIMO systems for physical channel models", *IEEE ICASSP*, pp. 3464-3467, May 2011.

[7] T. E. Bogale and L. B. Le "Pilot optimization and channel estimation for multiuser massive MIMO systems", *IEEE CISS*, Mar. 2014.

[8] Papadopoulos, G. Caire and S. Ramprashad, "Achieving large spectral efficiencies from MU-MIMO with tens of antennas: location adaptive TDD MU-MIMO design and user scheduling", *IEEE ASILOMAR*, pp. 636-643, Nov. 2010.

[9] H. Huh, G. Caire, Papadopoulos, Ramprashad "Achieving "Massive MIMO" Spectral Efficiency with a Not-so-Large Number of Antennas," *IEEE Trans. on Wireless Communications*, vol.11, no.9, pp.3226-3239, September 2012

[10] K. Appaiah, A. Ahsikhmin and T. Marzetta, "Pilot contamination reduction in multi-user TDD systems," *IEEE ICC*, May 2010.

[11] Y. Li, Y.-H. Nam, B. l. Ng and J. Zhang "A non-asymptotic throughput for massive MIMO cellular uplink with pilot reuse," *Wireless Communication Symposium - Globecom*, pp. 4500-4504, 2012.

[12] G. L. Stuber, *Principles of Mobile Communication*, 2nd ed. NYC, NY, USA: Springer, 2011.